Max-Planck-Institut für Meteorologie
Max Planck Institute for Meteorology

Report No. 336

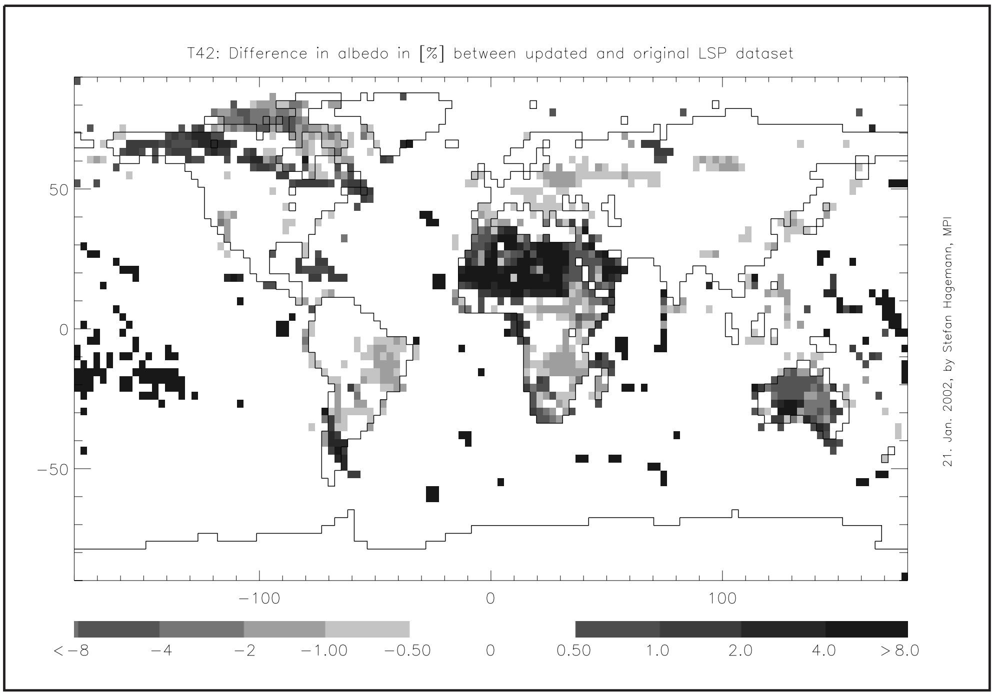

An Improved Land Surface Parameter Dataset for Global and Regional Climate Models

by

Stefan Hagemann

Hamburg, January 2002

Authors

Stefan Hagemann

Max-Planck Institut für Meteorologie
Hamburg

Max-Planck-Institut für Meteorologie
Bundesstrasse 55
D - 20146 Hamburg
Germany

Tel.: +49-(0)40-4 11 73-0
Fax: +49-(0)40-4 11 73-298
e-mail: <name>@dkrz.de
Web: www.mpimet.mpg.de

AN IMPROVED LAND SURFACE PARAMETER DATASET FOR GLOBAL AND REGIONAL CLIMATE MODELS

STEFAN HAGEMANN

Max Planck Institute for Meteorology
Bundesstraße 55
D-20146 Hamburg, Germany

*e-mail: Hagemann@dkrz.de
http://www.mpimet.mpg.de/privat/Mitarbeiter/hagemann.stefan
Tel.: +49-40-41173-101
Fax: +49-40-41173-366

MPI Report 336

January 2002

ISSN 0937-1060

Contents

Abstract

In 1999, *Hagemann et al.* derived a global dataset of land surface parameters (LSP) from a global distribution of major ecosystem types that was made available by the U.S. Geological Survey. These parameters are: background surface albedo, surface roughness length due to vegetation, fractional vegetation cover and leaf area index for the growing and dormancy season, forest ratio, plant-available and total soil water holding capacity. The LSP dataset is provided for the use in global and regional climate modelling and it was successfully implemented in the regional climate models HIRHAM and REMO as well as in the global ECHAM model.

As the U.S. Geological Survey has recently made an updated version of their ecosystem dataset available, these changes were incorporated in the LSP dataset. During this implementation, several improvements were made to the LSP dataset. Over Africa, the background surface albedo of bare soil was corrected with METEOSAT albedo data. In addition, the seasonal variation of vegetation characteristics was considered and monthly mean fields of vegetation ratio, leaf area index and background albedo were developed and implemented.

1. Introduction

For an adequate modelling of climate, an accurate representation of the land surface characteristics is required. As stated in a review by *Rowntree* (1991), numerous climate simulations have shown that anomalies in albedo and surface roughness can produce significant changes in the atmospheric circulation. *Pielke et al.* (1997) have demonstrated that the landscape, including its spatial heterogeneity, has a substantial influence on the overlying atmosphere. An adequate determination of land surface characteristics dependent on plant canopies is of particular importance because they strongly modify the evapotranspiration over large areas of the land surface which is a major component of the surface thermal and moisture balance and of the hydrological cycle. Thus the assessment of new or improved land surface datasets was central to a number of programs and experiments, e. g. the 'International Satellite Land-Surface Climatology Program' (ISLSCP) and the 'International Geosphere-Biosphere Program' (IGBP). For an overview about these programs and experiments, see *Feddes et al.* (1998).

As mentioned by *Hagemann et al.* (1999), several global land surface parameter datasets exist but the available datasets are inaccurate in some regions of the world and, generally, their spatial resolution is too coarse to fit the demands of high resolution limited area models. Recent development in remote sensing facilitated the measurement of present land surface characteristics at a very fine spatial resolution thereby offering the possibility to create consistent land surface boundary conditions for numerical models.

Hagemann et al. (1999) have constructed a global dataset of land surface parameters (LSP) which is based on a 1 km global distribution of major ecosystem types (*Loveland et al.*, 2000) including glacial ice and open water according to the definitions given by *Olson* (1994a, 1994b). The latter was made available by the *U.S. Geological Survey* (1997). The set of the chosen parameters of the LSP dataset (background surface albedo, surface roughness length due to vegetation, fractional vegetation cover and leaf area index for the growing and dormancy season, forest ratio, plant-available and total soil water holding capacity) was defined by the parameters that are used or shall be used in the climate models of the Max Planck Institute for Meteorology (MPI). The global LSP dataset is available for use in regional and global climate modelling and it is implemented in the regional climate models HIRHAM (*Christensen et al.*, 1996) and REMO (*Jacob*, 2001) as well as in the global ECHAM model (*Roeckner et al.*, 1996).

From the basic resolution of 1 km the parameter values can be aggregated to the respective model resolution (see *Hagemann et al.*, 1999). Due to the finest resolution of 1 km that may be obtained, the LSP dataset has been shown to be very suitable for the application in very high resolution regional climate modelling as it was done with the HIRHAM model (*Christensen et al.*, 2001; *Hagemann et al.*, 2001) and the REMO model (*Rechid*, 2001). But the implementation of the LSP dataset in the global ECHAM model has also led to improvements in the simulation of the hydrological cycle at the coarse resolution of T42 (about 2.8°) as shown in *Hagemann et al.* (2000).

This technical note describes the changes and improvements that were made since the first publication of the LSP dataset by *Hagemann et al.* (1999). The technical changes to the dataset are described in Sect. 2, and Sect. 3 gives a short comparison of the updated LSP dataset to its first version.

2. Changes in the land surface parameters

In this section, the technical changes in the LSP dataset are described. This includes the changes in the dataset of major ecosystem types (Sect. 2.1), the changes in the allocation of parameter values to the ecosystem types (Sect. 2.2), the correction of the bare soil surface albedo over Africa using independent satellite data (Sect. 2.3), and the implementation of a monthly seasonal variation of the vegetation (Sect. 2.4).

2.1. Changes in the global 1 km distribution of major ecosystem types

As mentioned in Sect. 1, the *U.S. Geological Survey* (1997) has constructed their global 1 km distribution of major ecosystem types (Global Land Cover Characteristics Database; GLCCD) according to a classification list of *Olson* (1994a, 1994b). For Version 2.0 (U.S. Geological Survey, 2001), land cover classes over 10% of the earth‘s land area were revised. Key revision focus areas included: boreal forest transition zone, forest/cropland separation in Europe, Miombo forest in Africa, Amazon rainforest.

In the first version of GLCCD, only 70 of the 94 ecosystem types from Olson classification list are included (see Table 1). In GLCCD Version 2, two new ecosystem types are added (*Evergreen Tree Crop*, *Deciduous Tree Crop*) to the list (see Table 2) and included in the dataset. Water gridboxes are now separated into *Inland Water* and *Sea Water*. Several gridboxes are now classified as *Wet Sclerophylic Forest*, and *Dry Evergreen Woods* does not occur anymore. Several 1 km gridboxes are classified as missing data. From the global distribution of these gridboxes they can be recognized as land points mostly surrounded by water. Thus, these gridboxes are defined as the new ecosystem type *Small Islands*.

2.2. Changes in the allocation of parameter values to the ecosystem types

A revised judgement of the ecosystem types caused changes in the surface albedo and vegetation roughness length values of several mixed crops/fields ecosystem types (19, 30, 31, 55, 56, 57, 58, 93). These changes are in agreement with proposed changes suggested by *Jacob* (personal communication, 2001). Parameter values for the new ecosystem types (cf. Sect. 2.1) are defined based on *Claussen et al.* (1994). For all ecosystem types, the values of vegetation ratio and leaf area index for both growing and dormancy season are revised and partially corrected using a distribution of fraction of photosynthetic absorbed radiation f_{PAR} *(Knorr,* 1997, 1998) as described in *Hagemann et al.* (1999). For land use types where the vegetation ratio is corrected, the corresponding forest ratio is corrected in an analogous way. Due to weaknesses in the forest coverage over Scandinavia (e.g. *Raschke*, *Graham*, personal communication, 1999), the old values of *Claussen et al.* (1994) are used for the vegetation ratio and forest ratio of *Conifer Boreal Forest* over Scandinavia. Also a typing error in the leaf area index for *Cold Grassland* in the dormancy (0.) and growing season (2.89) is corrected. The method to derive typical values of plant available water capacity and volumetric wilting point was repeated for each ecosystem type as described in *Hagemann et al.* (1999).

2.3. Surface albedo correction over Africa

In the LSP dataset, each parameter distribution is based only on the allocation of parameter values to land use types. This offers the possibility to easily derive different parameter distributions by changing the land use types distribution as it may be desired in experiments using different (e. g. future or paleo-climatic) boundary conditions. But over bare soil regions, such as deserts, the background (surface) albedo over snow-free land α_s depends on the soil type and colour. Differences in these soil characteristics are not represented by differences in ecosystem types. This has lead to significant deviations from satellite derived albedo values over desert regions, in particular. Systematic errors in the surface albedo of larger bare soil areas may have a significant influence on the quality of climate simulations over these regions, as shown by *Knorr et al.* (2001) for North Africa.

To overcome this problem, *Claussen et al.* (1994) have merged their 0.5 degree albedo dataset with 2.5 degree surface albedo data which were derived from observed clear sky albedo data of the ‘Earth Radiation Budget Experiment‘ (ERBE; *Ramanathan et al.*, 1989) using ECHAM3 (*Roeckner et al.*, 1992) for estimating the atmospheric correction. This method is considered as too uncertain and the resolution of 2.5˚ is too coarse to fit the demands of high resolution applications, so that a merging of the LSP albedo with the ERBE data was not adopted. Instead we use Meteosat surface albedo (MSA) data (*Knorr et al.*, 2001) which were recently made available over Africa and southern Europe at the comparatively high resolution of 8 km. These data were derived from half-hourly visible band data of the Meteosat-5 radiometer and presented by *Pinty et al.* (2000). As they have used a more refined method to derive surface albedo data at a resolution that fits the demand of high resolution applications, the MSA data are used to correct the LSP albedo values α_{lsp}. In order to be consistent to the other vegetation data, only the bare soil part of a grid box is replaced by MSA values α_{msa} (cf. *Claussen et al.*, 1994). Thus, the surface albedo α_s is computed as a blend of α_{lsp} and α_{msa} according to

$$\alpha_s = \alpha_{msa} \cdot (1 - c_v) + \alpha_{lsp} \cdot c_v \qquad (1)$$

Here, c_v designates the vegetation ratio within a gridbox. (Technically the blend of the two albedo data is computed after the aggregation of the LSP albedo to the target resolution was conducted.) As can be obtained from Fig. 3b, the MSA data seem to have unrealistic values in some regions north of 40˚N. Therefore, the LSP albedo is only corrected between 40˚S and 40˚N.

2.4. Seasonal variation of the vegetation

The parameters in the first version of the LSP dataset represent annual mean values of land surface characteristics. Now, the seasonal variation of vegetation characteristics is provided (see also *Christensen et al.*, 2001). Monthly mean fields of vegetation ratio, leaf area index and background albedo were developed and implemented. The fields of vegetation ratio and LAI are based on the minimum and maximum values of fractional vegetation cover and leaf area index from LSP dataset, monthly values of fraction of absorbed photosynthetically active radiation FPAR (*Knorr*, 1998), and a monthly 2m temperature climatology TLW (*Legates and Wilmott*, 1990). The datasets of FPAR and TLW are used to define a global field of a monthly growth factor f_i which determines the growth characteristics of the vegetation at a resolution of 0.5 degree. This growth factor represents the local climate and it does not vary largely between grid boxes in a certain climate region. Thus it can be aggregated to coarser resolutions and may also be applied to data with higher resolutions than 0.5 degree without a significant loss of information.

Since FPAR is a direct measure of the amount of vegetation on the land surface, it is used for the definition of the growth factor f_i in all grid boxes where a FPAR value is available in all 12 months of the year. This comprises merely the low and mid-latitudes since in high latitudes, no FPAR values are available throughout the year due to snow coverage and the run of the satellite orbit. For a certain grid box, f_i is defined by

$$f_i = 1 - \left(\frac{FPAR_{max} - FPAR_i}{FPAR_{max} - FPAR_{min}}\right)^2 \tag{2}$$

$FPAR_i$ is the FPAR value of month i, $FPAR_{min}$ and $FPAR_{max}$ are the minimum and maximum monthly FPAR values for the grid box, respectively. In high latitudes, the growth of the vegetation is mainly limited by temperature. Here, TLW is used and f_i is defined by

$$f_i = 1 - \left(\frac{T_{max} - T_i}{T_{max} - T_{min}}\right)^2 \tag{3}$$

T_i is the climatological 2m temperature of month i. In high latitudes, it is assumed that the minimum vegetation is present for temperatures below T_{min} = 278 K and the maximum vegetation is present at the maximum monthly 2m temperature T_{max} or for temperatures above T_{max} = 298 K, whichever is lower. Using the growth factor f_i based on Eq. (2) and (3), the monthly LAI_i (analogous for the vegetation ratio) can be computed as

$$LAI_i = LAI_{min} + f_i \cdot (LAI_{max} - LAI_{min}) \tag{4}$$

The background albedo α_i of month i is derived from the LAI_i of month i based on *Zeng et al.* (1999):

$$\alpha_i = \alpha_0 - c \cdot (1 - e^{-0.5 \cdot LAI_i}) \qquad (5)$$

c is set to a default of 0.15 and α_0 is computed from Eq. (5) inserting the annual averages of albedo and LAI from LSP dataset. Both *c* and α_0 are corrected to achieve minimum albedo values (corresponding to the maximum LAI) of 0.09 (*Zeng*, personal communication, 2000) where the annual mean albedo is above 0.09, thereby retaining the same annual mean albedo.

As an example for the seasonal varying vegetation fields, Fig. 1 shows the vegetation ratio at T42 resolution (about 2.8˚) for the months January, April, July and October as used in the ECHAM model. Here, the vegetation ratio is related only to the land part of a gridbox (In contrast to the standard definition where its value corresponds to the fraction of vegetated area in the whole gridbox.).

3. Discussion of the updated LSP dataset

In this section, the updated version of the LSP dataset is compared to its first version. The comparison is done from a global point of view at 0.5 degree resolution.

In Fig. 2, the surface background albedo is shown for the first and the updated version of the LSP albedo without MSA correction. In the latter, the most apparent changes occur over Australia. Although the MSA correction was conducted only over the bare soil part, the final updated version of the LSP albedo agrees quite well with the MSA over Africa, Saudi Arabia and the parts of Europe south of 40˚N (Fig. 3).

For the vegetation roughness length, the most apparent changes occur over Australia, India, Alaska, South and Central Europe (Fig. 4). Especially over Europe the changes are primarily caused by the revised values assigned to several mixed crops/fields ecosystem types (cf. Sect. 2.2).

For the total (field capacity, not shown) and the plant-available soil water-holding capacity (Fig. 5), the largest changes occur over eastern Europe, Tibetan plateau, East Africa, the Sahel zone and Australia. These changes are related to the redistribution of ecosystem types in the GLCCD dataset (see Sect. 2.1) and the different allocation of typical values to the ecosystem types caused by this redistribution.

As stated in Hagemann et al. (1999), FPAR can be expressed as a function of vegetation ratio and LAI. A comparison of the growing season FPAR values computed for both versions of the LSP dataset to the maximum FPAR distribution of *Knorr* (1997, 1998) is shown in Fig. 6. Large improvements in the updated LSP dataset can be seen over Australia and Central Africa. Also over north-west part of North America and northern Eurasia, the updated FPAR values are generally closer to the FPAR data of *Knorr* (1997, 1998) than the original FPAR values.

One general weakness of the 1 km satellite data is the inadequate allocation of wetlands. This may be caused by the fact that the ecosystem types are allocated according to the major features of vegetation and land use. Thus, regions where the wetlands are only a secondary feature are not well characterized. In the GLCCD Version 2, the Pantanal swamps and the wetlands in the Parana catchment in South America are still not well represented. The same applies to the wetlands in the Congo basin and in the East African highland lake area. Only the representation of the wetlands surrounding the southern Hudson Bay is improved.

An accurate separation of lakes from the land ecosystem types is possible since a global distribution of fraction of land (or water) may be directly derived from the 1 km global dataset of ecosystem types (not shown). But the situation is different for wetlands. The currently best available global dataset for hydrological modelling that describes the fractional coverage by wetlands is a dataset of *Matthews and Fung* (1987) as indicated by results of *Hagemann and Dümenil* (1997). This dataset has a resolution of 1 degree which is certainly too coarse for regional climate modelling. An opportunity for the future may be the merging of this dataset with a wetlands distribution derived from the 1 km global ecosystem data.

4. Summary

An improved version of the LSP dataset of *Hagemann et al.* (1999) is presented. The LSP dataset is based on the GLCCD distribution of major ecosystem types (*U.S. Geological Survey*, 1997). The incorporation of GLCCD version 2 (*U.S. Geological Survey*, 2001), where about 10% of the land cover classes have changed, leads to differences in the parameter distributions of the LSP dataset, especially over Australia, the boreal forest transition zone, and over areas with mixed forest/cropland types. Smaller differences arise from changes in the parameter allocation to the ecosystem types, such as, e.g., for the vegetation roughness length over Central Europe. The overall distribution of vegetation (with regard to vegetation ratio and leaf area index) seems to be improved compared to *Knorr* (1997, 1998) in the updated LSP dataset.

The MSA correction of the bare soil surface albedo leads to a more realistic representation of the surface albedo over Africa and Saudi Arabia. While the parameters in the first version of the LSP dataset represent annual mean values of land surface characteristics, the inclusion of a seasonal cycle of vegetation ratio, leaf area index and surface albedo may improve the simulation of the seasonal cycle in climate models.

The updated LSP dataset is still subject to improvements in some cases, especially regarding coarse resolution GCM applications. The soil water capacity distribution may be improved by using soil type information such as the 0.5 degree soil type dataset of *Dunne and Wilmott* (1996) based on *FAO/Unesco* (1971-1981). Although very high resolution soil type data are currently not globally available, the existing data may be used to correct the W_{cap} data for coarse resolution GCM applications. As it was done in the Sahara and Saudi Arabia using the METEOSAT albedo data, soil surface albedo information would be useful to improve the background albedo distribution in other bare soil regions.

The Danish Meteorological Institute has planned to construct also a seasonal distribution of vegetation roughness length for the implementation into the HIRHAM model (*Christensen*, personal communication, 2001) which will be incorporated into the LSP dataset afterwards.

Acknowledgements

I thank Daniela Jacob from the MPI for fruitful discussions about vegetation roughness length data. I am also grateful to Jens Hesselberg Christensen and Ole Bossing Christensen from the Danish Meteorological Institute for their close cooperation in testing the LSP dataset in HIRHAM. I wish to thank Wolfgang Knorr from the MPI who has provided the METEOSAT albedo data. I appreciate the help of Monika Esch and Uwe Schulzweida from the MPI who implemented the LSP dataset into the ECHAM model and who have performed several ECHAM simulations during the test phase of the dataset. To Erich Roeckner from the MPI, I want to give thanks for valuable discussions about the results of the ECHAM simulations.

References

Christensen, J.H., Christensen, O.B., Lopez, P., van Meijgaard, E., and Botzet, M., 1996
The HIRHAM 4 regional atmospheric climate model
DMI Scientific Report **96-4**, Copenhagen, Denmark

Christensen, J.H., Christensen, O.B., Schulz, J-P., Hagemann, S., and Botzet, M., 2001
High resolution physiographic data set for HIRHAM 4: An application to 50 km horizontal resolution domain covering Europe
DMI, Technical Report **01-15 4**
(Available from DMI, Lyngbyvej 100, DK-2100 Copenhagen Ø).

Claussen, M., U. Lohmann, E. Roeckner and U. Schulzweida, 1994
A global dataset of land surface parameters
Max-Planck-Institute for Meteorology, Report **135**, Hamburg, Germany

Dunne, K.A., and C.J. Wilmott, 1996
Global distribution of plant-extractable water capacity of soil
Int. J. Climatol. **16**, 841-859

FAO/Unesco, 1971-1981
Soil map of the world
Vols. 1-10, Unesco, Paris

Feddes, R.A., P. Kabat, A.J. Dolman, R.W.A. Hutjes and M.J. Waterloo, 1998
Large-scale field experiments to improve land surface parameterisations
In: R. Lemmelä and N. Helenius (Eds.): Proceedings of ‘The Second International Conference on Climate and Water‘, Espoo, Finland, 17-20 August 1998: 619-646

Hagemann, S., and L. Dümenil, 1997
Comparison of two global wetlands datasets
In: G. Cecchi, E.T. Engman and E. Zilioli (Ed.), Earth Surface Remote Sensing
Proceedings of SPIE **3222**, 193-200

Hagemann, S., Botzet, M., Dümenil, L., and Machenhauer, B.,1999
Derivation of global GCM boundary conditions from 1 km land use satellite data
Max-Planck-Institute for Meteorology, Report **289**, Hamburg, Germany.
(Report available electronically from: http://www.mpimet.mpg.de/deutsch/Sonst/Reports/HTMLReports/289/)

Hagemann, S., M. Botzet, L. Dümenil Gates and B. Machenhauer, 2000
Impact of new global land surface parameter fields on ECHAM T42 climate simulations
In: H. Ritchie (Ed.), Research Activities in Atmospheric and Oceanic Modelling, Report 30
WMO/TD **987**, WMO, Geneva

Hagemann, S., Botzet, M., and Machenhauer, B., 2001
The summer drying problem over south-eastern Europe: Sensitivity of the limited area model HIRHAM4 to improvements in physical parameterization and resolution
Physics and Chemistry of the Earth, *Part B*, **26**, 391-396

Jacob, D. (2001) A note to the simulation of the annual and inter-annual variability of the water budget over the Baltic Sea drainage basin, *Meteorology and Atmospheric Physics* **77**, 61-73

Knorr, W., 1997
Satellitengestützte Fernerkundung und Modellierung des globalen CO_2-Austauschs der Landvegetation: Eine Synthese

Examensarbeit 49, Max-Planck-Institute for Meteorology, Hamburg, Germany

Knorr, W., 1998
Constraining a global mechanistic vegetation model with satellite data.
In: ‘IEEE International Geosciency and Remote Sensing Symposium‘ Proceedings, Seattle, WA, 6-10 July 1998.

Knorr, W., K.-G. Schnitzler and Y. Govaerts, 2001
The role of bright desert regions in shaping North African climate
Geophys. Res. Lett., accepted

Legates, D.R., and Willmott, C.J., 1990
Mean seasonal and spatial variability in global surface air temperature, *Theor. Appl. Climatol.* **41**, 11-21

Loveland, T.R., Reed, B.C., Brown, J.F., Ohlen, D.O., Zhu, J, Yang, L., and Merchant, J.W., 2000,
Development of a Global Land Cover Characteristics Database and IGBP DISCover from 1-km AVHRR Data, *Int. J. Remote Sens.* **21**, 1303-1330

Matthews, E., and I. Fung, 1987
Methane emissions from natural wetlands: Global distribution, area, and environmental characteristics of sources
Global Biogeochem. Cycles **1**, 61-86

Olson, J.S., 1994a
Global ecosystem framework-definitions
USGS EROS Data Center Internal Report, Sioux Falls, SD

Olson, J.S., 1994b
Global ecosystem framework-translation strategy
USGS EROS Data Center Internal Report, Sioux Falls, SD

Pielke, R.A., T.J. Lee, J.H. Copeland, J.L. Eastman, C.L. Ziegler and C.A. Finley, 1997
Use of USGS-provided data to improve weather and climate simulations
Ecological Applications **7** (1): 3-21

Pinty, B., F. Roveda, M.M. Verstraete, N. Gobron, Y. Govaerts, J.V. Martonchik, D.J. Diner, and R.A. Kahn, 2000
Surface albedo retrieval from Meteosat - 2. Applications
J. Geophys. Res. **105**, 18113-18134

Ramanathan, V., R.D. Cess, E.F. Harrison, P. Minis, B.R. Barkstrom, E. Ahmad and D. Hartmann, 1989
Cloud-radiative forcing and climate: results from the Earth Radiation Budget Experiment
Science **243**: 57-63

Rechid, D., 2001
Untersuchung zur Parameterisierung von Landoberflächen im regionalen Klimamodell REMO
Diplomarbeit, Max-Planck-Institute for Meteorology, Hamburg

Roeckner, E. , K. Arpe, L. Bengtsson, S. Brinkop, L. Dümenil, M. Esch, E. Kirk, F. Lunkeit, M. Ponater, B. Rockel, R. Sausen, U. Schlese, S. Schubert and M. Windelband, 1992
Simulation of the present-day climate with the ECHAM model: Impact of model physics and resolution
Max-Planck-Institute for Meteorology, Report **93**, Hamburg, Germany

Roeckner, E., K. Arpe, L. Bengtsson, M. Christoph, M. Claussen, L. Dümenil, M. Esch, M. Giorgetta, U. Schlese and U. Schulzweida, 1996
The atmospheric general circulation model ECHAM-4: model description and simulation of present-day climate
Max-Planck-Institute for Meteorology, Report **218**, Hamburg, Germany

Rowntree, P.R., 1991
Atmospheric parameterization schemes for evaporation over land: basic concepts and climate modelling aspects
In: Schmugge, T.J. and J. Andre (Eds.): *Land Surface Evaporation - Measurement and Parameterization*, Springer Verlag, S. 5-29

U.S. Geological Survey, 1997
Global land cover characteristics data base
http://edcwww.cr.usgs.gov/landdaac/glcc/globe_int.html

U.S. Geological Survey, 2001
Global land cover characteristics data base version 2.0
http://edcdaac.usgs.gov/glcc/globdoc2_0.html

Zeng, N., J.D. Neelin, W.K.-M. Lau, and C.J. Tucker, 1999
Enhancement of interdecadal climate variability in the Sahel by vegetation interaction
Science **286**, 1537-1540

Table 1: Parameter values according to *Hagemann et al.* (1999)

Global ecosystem types of *Olson* (1994a, 1994b) not occurring in the first version of the GLCCD dataset are excluded from the table. The parameters are background surface albedo α_s, surface roughness length due to vegetation $z_{0,veg}$, fractional vegetation cover c_v and leaf area index *LAI* for the growing (g) and dormancy season (d), forest ratio c_f, plant-available soil water holding capacity W_{ava}, and volumetric wilting point f_{pwp}. W_{ava} is given in mm and $z_{0,veg}$ in m.

Type	Global Ecosystems Legend	α_s	$z_{0,veg}$	c_v g	c_v d	*LAI* g	*LAI* d	c_f	W_{ava}	f_{pwp}
1	Urban	0.2	2.5	0.	0.	0.	0.	0.	0.	0.48
2	Low Sparse Grassland	0.19	0.03	0.53	0.04	1.75	0.12	0.	580.	0.45
3	Coniferous Forest	0.13	1.	0.96	0.95	9.2	9.0	0.9	130.	0.41
4	Deciduous Conifer Forest	0.13	1.	0.56	0.	3.6	0.1	0.56	155.	0.45
5	Deciduous Broadleaf Forest	0.16	1.	0.88	0.	5.2	0.1	0.85	240.	0.53
6	Evergreen Broadleaf Forests	0.16	0.68	0.99	0.97	9.9	9.5	0.95	220.	0.38
7	Tall Grasses and Shrubs	0.2	0.1	0.7	0.26	2.2	0.76	0.	590.	0.35
8	Bare Desert	0.28	0.005	0.	0.	0.	0.	0.	100.	0.
9	Upland Tundra	0.17	0.03	0.64	0.07	2.3	0.4	0.	60.	0.33
10	Irrigated Grassland	0.16	0.03	0.9	0.1	4.5	0.	0.	450.	0.49
11	Semi Desert	0.28	0.005	0.1	0.	0.46	0.	0.	45.	0.51
12	Glacier Ice	0.7	0.005	0.	0.	0.	0.	0.	0.	0.
13	Wooded Wet Swamp	0.12	0.03	0.73	0.67	3.5	3.0	0.	235.	0.50
14	Water	0.07	0.0002	0.	0.	0.	0.	0.	0.	0.
16	Shrub Evergreen	0.165	0.55	0.6	0.22	6.	2.2	0.35	800.	0.46
17	Shrub Deciduous	0.16	0.26	0.45	0.08	4.6	0.45	0.22	140.	0.33
19	Evergreen Forest and Fields	0.16	0.25	0.78	0.3	6.	3.	0.3	200.	0.47
20	Cool Rain Forest	0.12	2.	0.96	0.96	9.3	9.3	0.95	70.	0.34
21	Conifer Boreal Forest	0.13	1.	0.5	0.5	5.5	5.5	0.44	185.	0.32
22	Cool Conifer Forest	0.13	1.	0.7	0.35	9.2	4.4	0.66	380.	0.49
23	Cool Mixed Forest	0.15	1.	0.95	0.02	4.2	0.1	0.95	140.	0.40
24	Mixed Forest	0.16	0.68	0.93	0.3	7.	1.	0.8	300.	0.51
25	Cool Broadleaf Forest	0.16	1.	0.88	0.17	5.2	0.51	0.85	210.	0.43
26	Deciduous Broadleaf Forest	0.16	1.	0.88	0.26	5.2	0.79	0.85	250.	0.51
27	Conifer Forest	0.13	1.	0.87	0.31	9.7	4.4	0.84	250.	0.49
28	Montane Tropical Forests	0.15	0.55	0.86	0.77	4.8	4.0	0.5	630.	0.47
29	Seasonal Tropical Forest	0.12	2.	0.99	0.71	9.1	2.74	0.98	200.	0.52
30	Cool Crops and Towns	0.18	0.1	0.9	0.36	2.5	1.85	0.	310.	0.50
31	Crops and Town	0.18	0.1	0.9	0.16	4.5	1.1	0.	450.	0.50
32	Dry Tropical Woods	0.14	0.55	0.96	0.22	6.1	2.5	0.63	470.	0.46
33	Tropical Rainforest	0.12	2.	0.96	0.96	9.3	9.3	0.95	235.	0.52
34	Tropical Degraded Forest	0.14	0.55	0.86	0.24	5.96	2.4	0.57	460.	0.50
35	Corn and Beans Cropland	0.18	0.1	0.9	0.08	2.5	0.4	0.	250.	0.495
36	Rice Paddy and Field	0.15	0.06	0.95	0.1	4.6	0.	0.	350.	0.49
37	Hot Irrigated Cropland	0.18	0.05	0.8	0.25	4.4	1.3	0.	390.	0.51
38	Cool Irrigated Cropland	0.18	0.05	0.6	0.	3.	0.	0.	370.	0.48
40	Cool Grasses and Shrubs	0.19	0.06	0.6	0.01	1.9	0.05	0.	480.	0.42
41	Hot and Mild Grasses & Shrubs	0.2	0.1	0.53	0.17	1.71	0.5	0.	680.	0.44
42	Cold Grassland	0.19	0.03	0.94	0.18	1.5	2.89	0.	270.	0.52
43	Savanna (Woods)	0.16	0.25	0.95	0.25	3.	0.91	0.4	900.	0.47
44	Mire, Bog, Fen	0.12	0.03	0.6	0.	2.5	0.1	0.	120.	0.38
45	Marsh Wetland	0.12	0.03	0.6	0.	2.5	0.1	0.	800.	0.55
46	Mediterranean Scrub	0.15	0.46	0.8	0.2	4.3	2.5	0.4	480.	0.54
47	Dry Woody Scrub	0.16	0.26	0.8	0.26	4.6	0.8	0.38	600.	0.47
48	Dry Evergreen Woods	0.18	0.04	0.6	0.3	1.8	1.7	0.53	400.	0.46
50	Sand Desert	0.28	0.005	0.	0.	0.	0.	0.	100.	0.
51	Semi Desert Shrubs	0.28	0.005	0.27	0.1	0.83	0.56	0.	500.	0.40
52	Semi Desert Sage	0.28	0.005	0.39	0.	1.18	0.	0.	860.	0.425
53	Barren Tundra	0.17	0.03	0.19	0.	1.89	0.	0.	60.	0.30
54	Cool South. Hemi. Mix-Forests	0.16	0.65	0.86	0.	4.8	0.1	0.8	80.	0.45
55	Cool Fields and Woods	0.19	0.1	0.9	0.2	3.	0.9	0.3	140.	0.445
56	Forest and Field	0.18	0.17	0.97	0.2	6.1	2.2	0.54	180.	0.47

Type	Global Ecosystems Legend	α_s	$z_{0,veg}$	c_v g	c_v d	LAI g	LAI d	c_f	W_{ava}	f_{pwp}
57	Cool Forest and Field	0.18	0.17	0.9	0.2	4.	1.	0.5	230.	0.485
58	Fields and Woody Savanna	0.19	0.1	0.95	0.28	5.1	2.1	0.32	620.	0.51
59	Succulent and Thorn Scrub	0.2	0.03	0.56	0.19	4.7	0.92	0.26	820.	0.43
60	Small Leaf Mixed Woods	0.15	1.	0.53	0.	3.69	0.1	0.53	240.	0.39
61	Deciduous & Mix. Boreal Forest	0.16	0.65	0.57	0.	4.7	0.1	0.53	140.	0.495
62	Narrow Conifers	0.15	0.31	0.53	0.	3.38	0.1	0.29	240.	0.34
63	Wooded Tundra	0.18	0.05	0.55	0.15	3.07	0.5	0.16	85.	0.35
64	Heath Scrub	0.2	0.1	0.5	0.	4.6	0.1	0.	90.	0.45
69	Polar and Alpine Desert	0.28	0.005	0.	0.	0.	0.	0.	35.	0.43
72	Mangrove	0.12	1.29	0.95	0.95	9.	9.	0.9	290.	0.50
76	Crop and Water Mixtures	0.15	0.06	0.65	0.12	4.4	0.16	0.	2000.	0.575
78	Southern Hemi. Mixed Forest	0.16	0.65	0.8	0.	4.7	0.1	0.75	235.	0.40
89	Moist Eucalyptus	0.16	0.65	0.85	0.55	4.8	2.8	0.8	270.	0.55
90	Rain Green Tropical Forest	0.12	2.	0.96	0.96	9.3	9.3	0.95	360.	0.42
91	Woody Savanna	0.16	0.25	0.53	0.33	1.9	1.06	0.4	490.	0.50
92	Broadleaf Crops	0.17	0.175	0.94	0.25	5.	2.3	0.31	360.	0.49
93	Grass Crops	0.185	0.065	0.72	0.	2.	0.	0.	140.	0.47
94	Crops, Grass, Shrubs	0.19	0.1	0.67	0.2	2.7	0.8	0.	490.	0.465

Table 2: Updated parameter values

Global ecosystem types of *Olson* (1994a, 1994b) not occurring in the second version of the GLCCD dataset are excluded from the table. The parameters are background surface albedo α_s, surface roughness length due to vegetation $z_{0,veg}$, fractional vegetation cover c_v and leaf area index *LAI* for the growing (g) and dormancy season (d), forest ratio c_f, plant-available soil water holding capacity W_{ava}, and volumetric wilting point f_{pwp}. W_{ava} is given in mm and $z_{0,veg}$ in m.

Type	Global Ecosystems Legend	α_s	$z_{0,veg}$	c_v g	c_v d	*LAI* g	*LAI* d	c_f	W_{ava}	f_{pwp}
1	Urban	0.2	2.5	0.	0.	0.	0.	0.	0.	0.48
2	Low Sparse Grassland	0.19	0.03	0.55	0.04	1.75	0.2	0.	580.	0.45
3	Coniferous Forest	0.13	1.	0.96	0.95	9.2	9.	0.9	130.	0.41
4	Deciduous Conifer Forest	0.13	1.	0.56	0.	3.7	0.1	0.56	155.	0.45
5	Deciduous Broadleaf Forest	0.16	1.	0.8	0.	5.1	0.1	0.8	300.	0.53
6	Evergreen Broadleaf Forests	0.16	0.68	0.96	0.95	9.9	9.5	0.95	200.	0.46
7	Tall Grasses and Shrubs	0.2	0.1	0.44	0.	1.5	0.1	0.	280.	0.50
8	Bare Desert	0.28	0.005	0.	0.	0.	0.	0.	100.	0.
9	Upland Tundra	0.17	0.03	0.51	0.	2.2	0.4	0.	120.	0.34
10	Irrigated Grassland	0.16	0.03	0.9	0.1	4.5	0.	0.	450.	0.49
11	Semi Desert	0.28	0.005	0.24	0.	0.7	0.	0.	300.	0.48
12	Glacier Ice	0.7	0.005	0.	0.	0.	0.	0.	0.	0.
13	Wooded Wet Swamp	0.12	0.03	0.73	0.67	3.4	3.	0.	235.	0.50
14	Inland Water	0.07	0.0002	0.	0.	0.	0.	0.	0.	0.
15	Sea Water	0.07	0.0002	0.	0.	0.	0.	0.	0.	0.
16	Shrub Evergreen	0.165	0.55	0.39	0.17	5.1	1.7	0.24	410.	0.45
17	Shrub Deciduous	0.16	0.26	0.53	0.1	4.6	0.5	0.26	350.	0.32
19	Evergreen Forest and Fields	0.16	0.45	0.85	0.4	6.	3.	0.5	200.	0.47
20	Cool Rain Forest	0.12	2.	0.96	0.96	9.3	9.3	0.95	80.	0.35
21	Conifer Boreal Forest	0.13	1.	0.52	0.52	6.	6.	0.46	140.	0.33
22	Cool Conifer Forest	0.13	1.	0.7	0.35	9.2	4.	0.66	380.	0.48
23	Cool Mixed Forest	0.15	1.	0.93	0.02	4.3	0.1	0.93	140.	0.40
24	Mixed Forest	0.16	0.68	0.97	0.3	7.	1.	0.83	220.	0.51
25	Cool Broadleaf Forest	0.16	1.	0.88	0.16	5.2	0.85	0.85	210.	0.43
26	Deciduous Broadleaf Forest	0.16	1.	0.95	0.19	5.3	0.95	0.92	320.	0.47
27	Conifer Forest	0.13	1.	0.87	0.31	9.7	4.	0.84	250.	0.49
28	Montane Tropical Forests	0.15	0.55	0.9	0.77	4.8	4.	0.52	700.	0.50
29	Seasonal Tropical Forest	0.12	2.	0.99	0.69	6.1	2.7	0.98	210.	0.53
30	Cool Crops and Towns	0.18	0.25	0.9	0.14	2.5	0.74	0.14	280.	0.475
31	Crops and Town	0.18	0.25	0.85	0.16	4.4	1.1	0.16	430.	0.50
32	Dry Tropical Woods	0.14	0.55	0.98	0.19	6.1	2.2	0.65	550.	0.44
33	Tropical Rainforest	0.12	2.	0.96	0.96	9.3	9.3	0.95	240.	0.52
34	Tropical Degraded Forest	0.14	0.55	0.87	0.24	6.	2.2	0.57	260.	0.52
35	Corn and Beans Cropland	0.18	0.1	0.9	0.08	2.5	0.4	0.	250.	0.495
36	Rice Paddy and Field	0.15	0.06	0.95	0.19	4.6	0.26	0.	350.	0.49
37	Hot Irrigated Cropland	0.18	0.05	0.83	0.28	4.4	1.4	0.	390.	0.51
38	Cool Irrigated Cropland	0.18	0.05	0.6	0.	3.	0.	0.	370.	0.48
40	Cool Grasses and Shrubs	0.19	0.06	0.59	0.01	1.8	0.05	0.	450.	0.44
41	Hot and Mild Grasses & Shrubs	0.2	0.1	0.58	0.16	1.85	0.85	0.	650.	0.40
42	Cold Grassland	0.19	0.03	0.98	0.02	3.	0.14	0.	260.	0.52
43	Savanna (Woods)	0.16	0.25	0.8	0.27	2.6	0.94	0.4	660.	0.485
44	Mire, Bog, Fen	0.12	0.03	0.67	0.	2.6	0.1	0.	160.	0.39
45	Marsh Wetland	0.12	0.03	0.85	0.	3.1	0.1	0.	800.	0.55
46	Mediterranean Scrub	0.15	0.46	0.8	0.66	4.3	0.28	0.4	620.	0.51
47	Dry Woody Scrub	0.16	0.26	0.34	0.2	4.	1.	0.2	610.	0.38
48	Dry Evergreen Woods	0.18	0.04	0.6	0.3	1.8	1.7	0.53	400.	0.46
50	Sand Desert	0.28	0.005	0.	0.	0.	0.	0.	100.	0.
51	Semi Desert Shrubs	0.28	0.005	0.24	0.08	0.73	0.41	0.	470.	0.40
52	Semi Desert Sage	0.28	0.005	0.39	0.	1.18	0.	0.	840.	0.425
53	Barren Tundra	0.17	0.03	0.14	0.	1.6	0.	0.	60.	0.31
54	Cool South. Hemi. Mix-Forests	0.16	0.65	0.81	0.	4.7	0.1	0.75	260.	0.38
55	Cool Fields and Woods	0.18	0.17	0.9	0.3	3.	0.76	0.3	180.	0.45

Type	Global Ecosystems Legend	α_s	$z_{0,veg}$	c_v g	c_v d	*LAI* g	*LAI* d	c_f	W_{ava}	f_{pwp}
56	Forest and Field	0.16	0.25	0.8	0.21	5.9	2.5	0.45	310.	0.50
57	Cool Forest and Field	0.16	0.25	0.9	0.2	4.1	1.	0.5	180.	0.50
58	Fields and Woody Savanna	0.18	0.17	0.95	0.35	5.	2.3	0.35	700.	0.48
59	Succulent and Thorn Scrub	0.2	0.03	0.85	0.24	4.7	0.9	0.4	740.	0.49
60	Small Leaf Mixed Woods	0.15	1.	0.47	0.	3.7	0.1	0.47	130.	0.43
61	Deciduous & Mix. Boreal Forest	0.16	0.65	0.64	0.	4.7	0.1	0.6	170.	0.46
62	Narrow Conifers	0.15	0.31	0.48	0.	3.4	0.1	0.27	180.	0.30
63	Wooded Tundra	0.18	0.05	0.47	0.15	3.1	0.5	0.34	100.	0.38
64	Heath Scrub	0.2	0.1	0.5	0.	4.6	0.1	0.	90.	0.45
69	Polar and Alpine Desert	0.28	0.005	0.	0.	0.	0.	0.	35.	0.43
72	Mangrove	0.12	1.29	0.95	0.95	9.	9.	0.9	290.	0.50
76	Crop and Water Mixtures	0.15	0.06	0.65	0.13	4.4	0.16	0.	2000.	0.575
78	Southern Hemi. Mixed Forest	0.16	0.65	0.93	0.34	5.	2.6	0.87	235.	0.46
79	Wet Sclerophylic Forest	0.16	0.65	0.87	0.5	4.8	2.6	0.8	300.	0.55
89	Moist Eucalyptus	0.16	0.65	0.75	0.59	4.7	3.1	0.7	210.	0.54
90	Rain Green Tropical Forest	0.12	2.	0.96	0.96	9.3	9.3	0.95	360.	0.42
91	Woody Savanna	0.16	0.25	0.95	0.32	1.9	1.	0.4	560.	0.485
92	Broadleaf Crops	0.17	0.175	0.95	0.12	5.	2.	0.3	240.	0.42
93	Grass Crops	0.185	0.1	0.91	0.2	2.5	1.1	0.2	240.	0.47
94	Crops, Grass, Shrubs	0.19	0.1	0.65	0.33	2.7	0.4	0.	530.	0.46
95	Evergreen Tree Crop	0.16	0.17	0.97	0.3	6.1	3.	0.5	250.	0.46
96	Deciduous Tree Crop	0.17	0.17	0.9	0.3	5.	2.	0.3	240.	0.51
100	Missing data (Small Islands)	0.2	0.03	0.53	0.2	4.1	1.	0.	180.	0.49

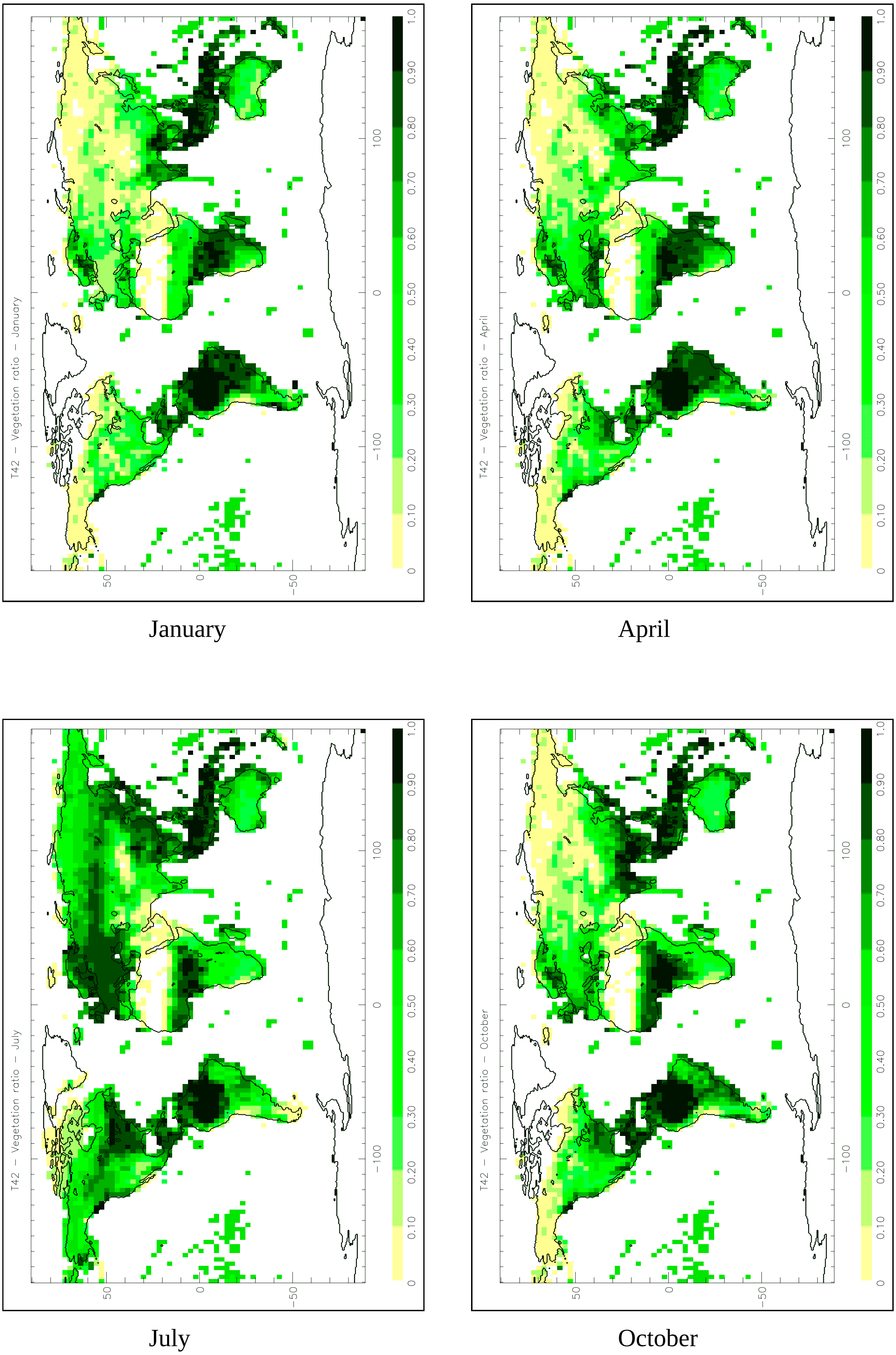

Fig. 1. Vegetation ratio of the updated LSP dataset at T42 resolution using the ECHAM5 definition where the ratio is related only to the land part of a gridbox. Gray scale in 10% steps.

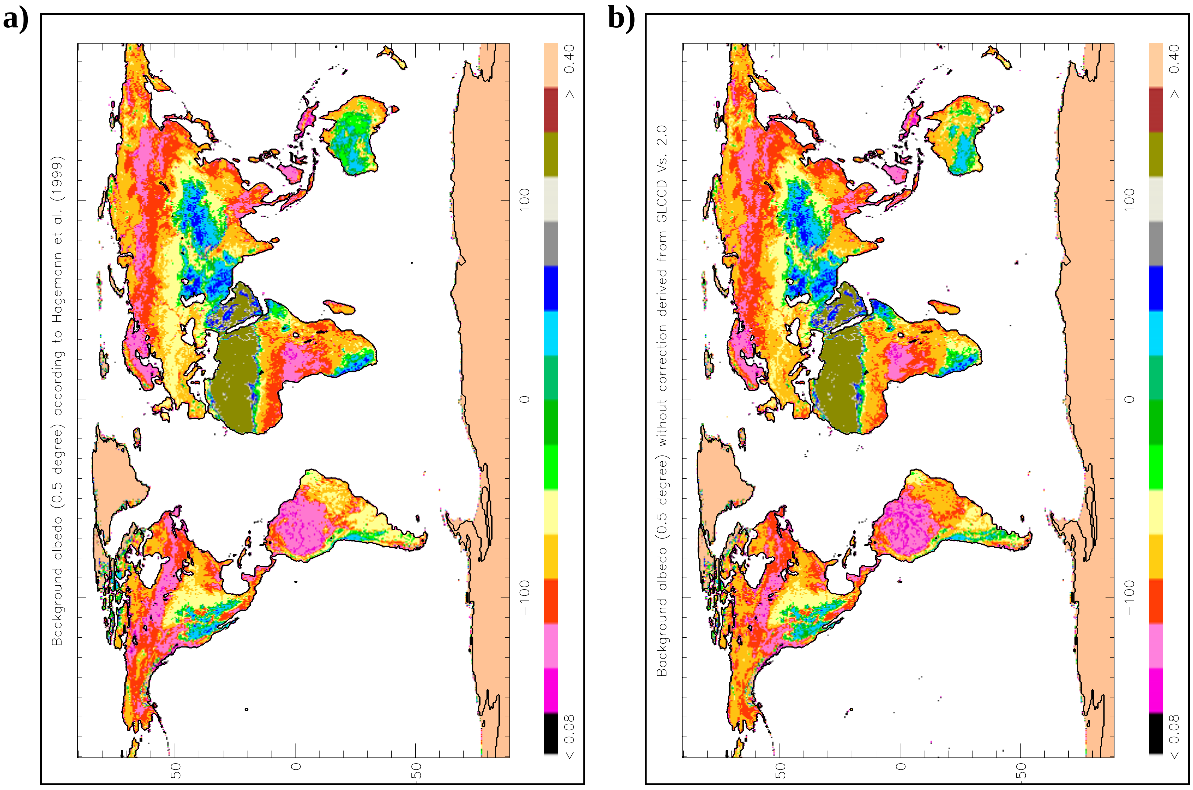

Fig. 2. Background albedo at 0.5 degree resolution **a)** according to *Hagemann et al.* (1999), and **b)** associated with GLCCD vs. 2 without albedo correction over Africa. Colour scale in 0.02 steps.

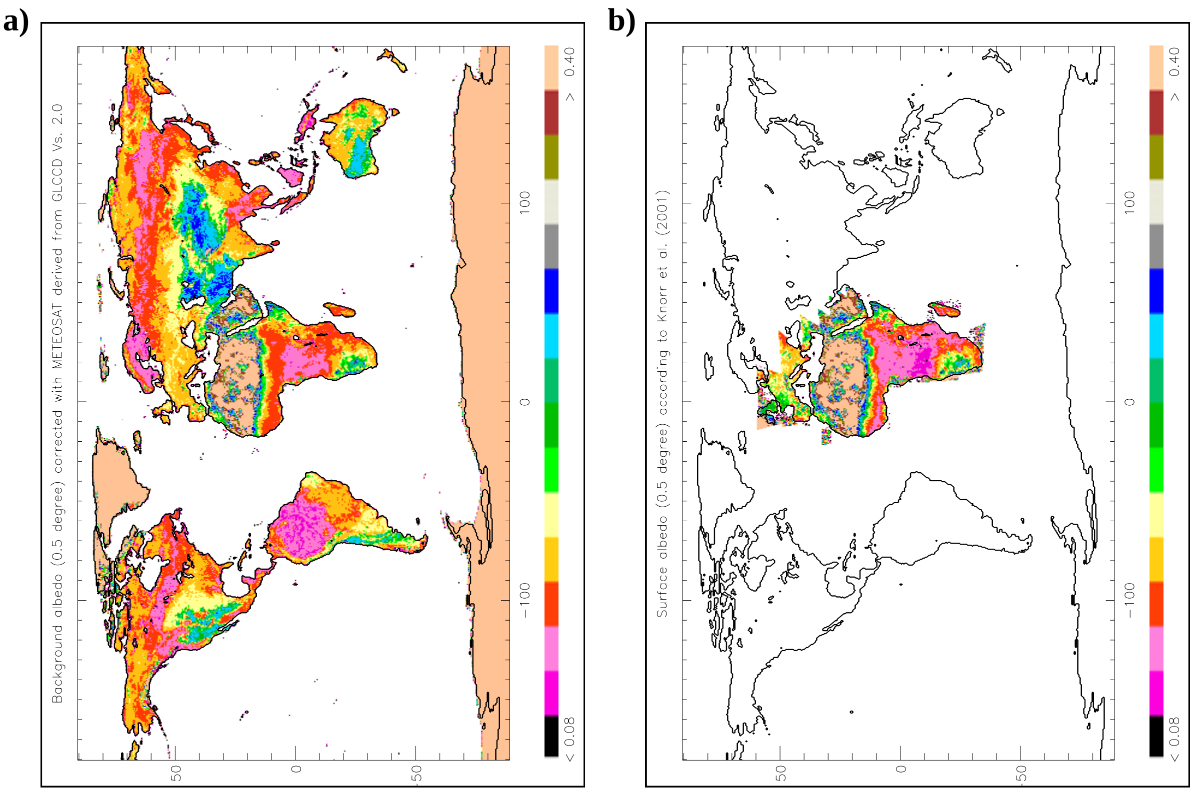

Fig. 3. a) Background albedo of the updated LSP dataset (corrected over Africa), and **b)** surface albedo according to *Knorr et al.* (2001) at 0.5 degree resolution. Colour scale in 0.02 steps.

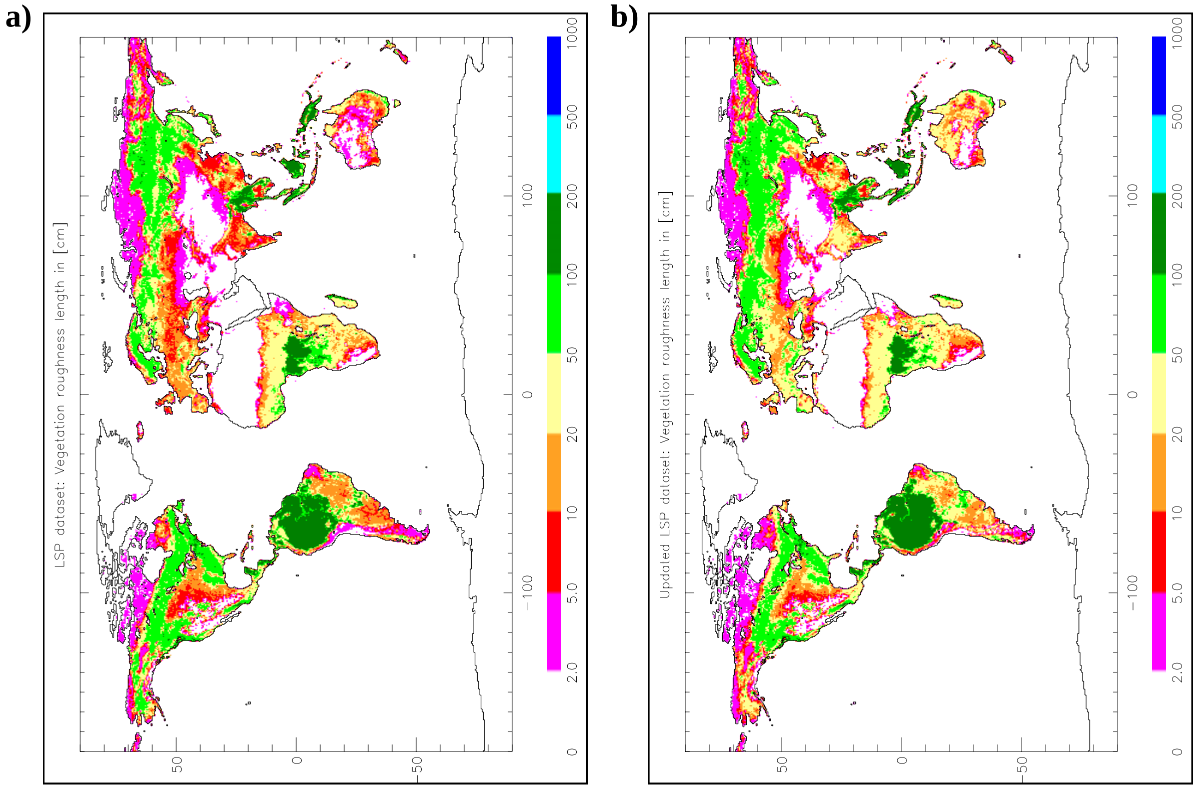

Fig. 4. Vegetation roughness length **a)** according to *Hagemann et al.* (1999) **b)** according to the updated LSP dataset at 0.5 degree resolution. Unit: cm.

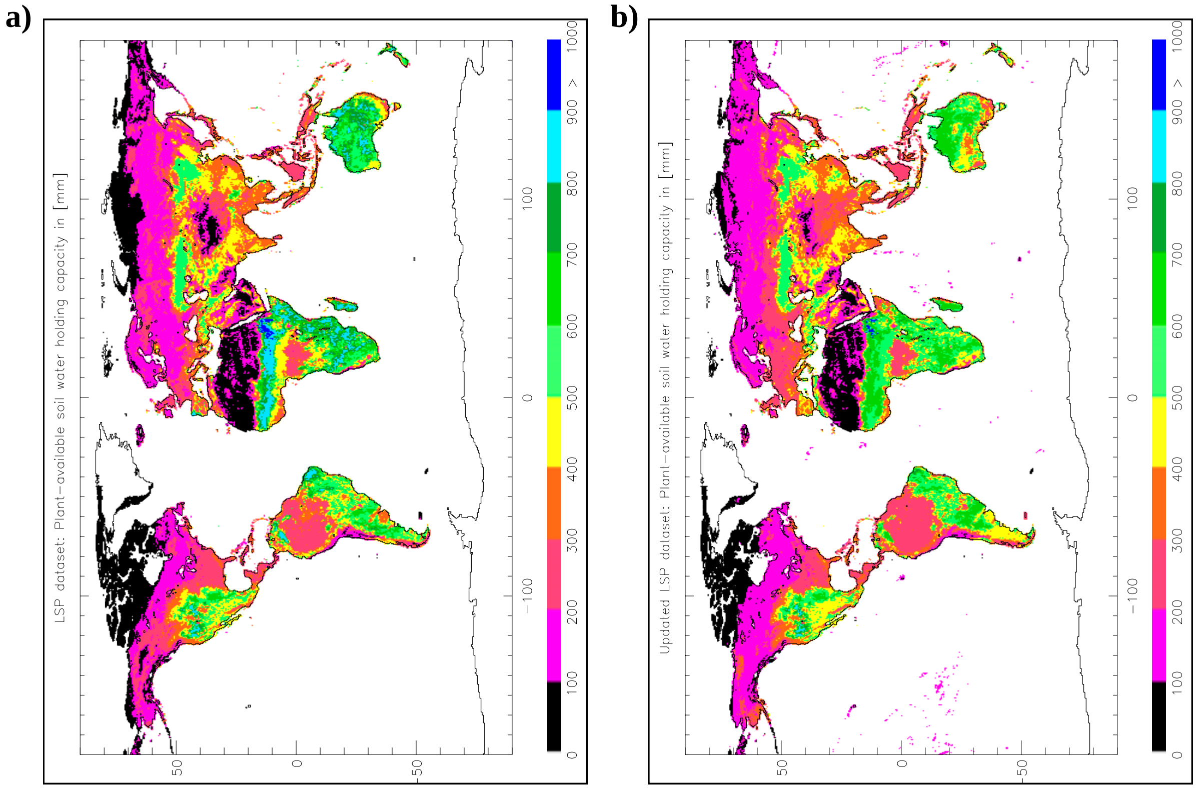

Fig. 5. Plant-available soil water holding capacity **a)** according to *Hagemann et al.* (1999) **b)** according to the updated LSP dataset at 0.5 degree resolution. Unit: cm.

a)

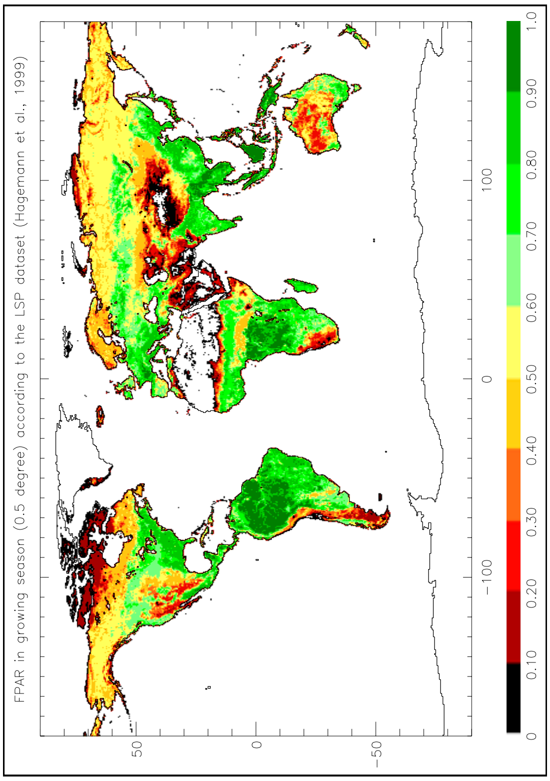

b)

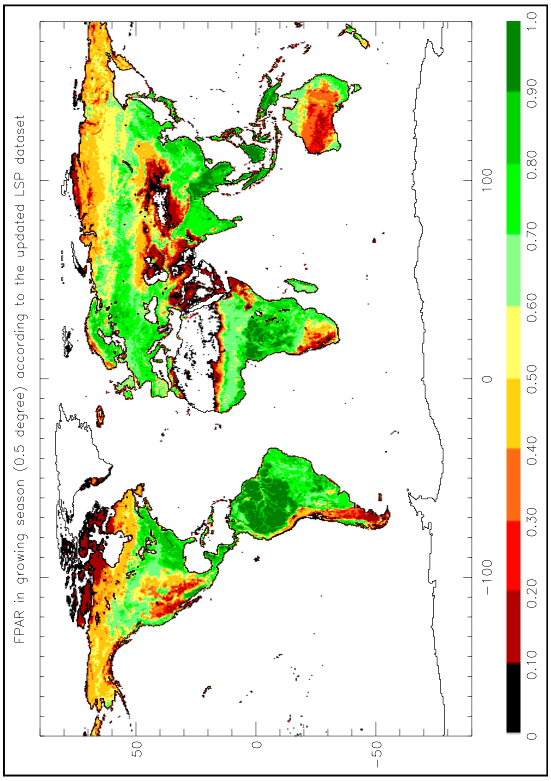

c)

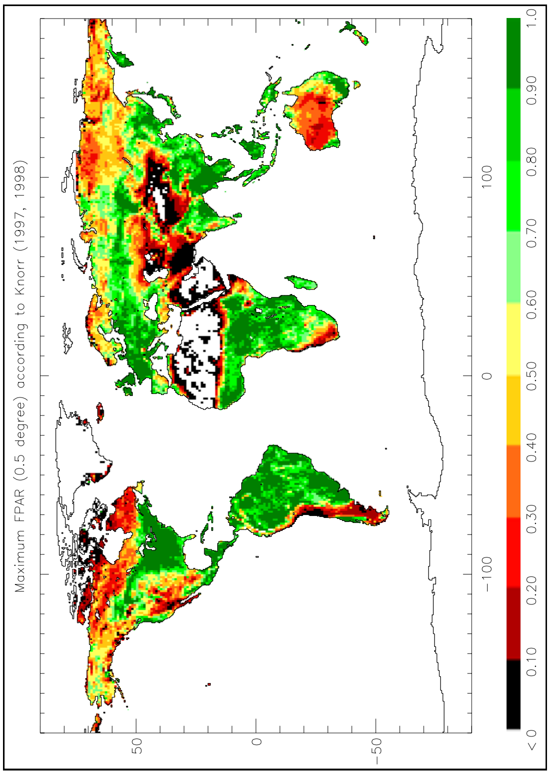

Fig. 6. f_{PAR} in the growing season at 0.5 degree resolution

a) according to *Hagemann et al.* (1999),
b) according to the updated LSP dataset, and
c) maximum f_{PAR} according to *Knorr* (1997, 1998).

Colour scale in 10% steps.